Available online at www.sciencedirect.com
ScienceDirect
Polymer 49 (2008) 1276–1284
polymer
www.elsevier.com/locate/polymer

Arborescent polystyrene-*graft*-poly(2-vinylpyridine) copolymers as unimolecular micelles: Solubilization studies

Gabriel Njikang, Mario Gauthier*, Jieming Li

Department of Chemistry, Institute for Polymer Research, University of Waterloo, 200 University Avenue West, Waterloo, Ontario N2L 3G1, Canada

Received 19 November 2007; accepted 5 January 2008
Available online 16 January 2008

Abstract

Solubilization of various polycyclic aromatic hydrocarbon (PAH) probes by arborescent polystyrene-*graft*-poly(2-vinylpyridine) unimolecular micelles of different structures in aqueous solutions was investigated by UV and fluorescence spectroscopies. The micelle–water partition coefficient K_w and the solubilization capacity κ^G both increased with the polystyrene content of the copolymers for all probes, but the increase was less significant for the less hydrophobic probes. The K_w values obtained correlated well with the octanol–water partition coefficient and the boiling point of the more hydrophobic probe molecules, but no clear trend was observed for κ^G. The results obtained suggest that highly hydrophobic probes are solubilized mainly in the non-polar polystyrene core. A significant portion of the least hydrophobic probes resides in the ionic shell, while probes of intermediate polarity appear to remain in the palisade (interfacial) region. The branching functionality of the micelles played an important role in the solubilization process: for copolymers of similar composition, the solubilization capacity and rate were lower for higher generations, presumably due to the more rigid structure of the molecules. The results obtained show that arborescent polystyrene-*graft*-poly(2-vinylpyridine) copolymers can be designed to solubilize compounds of different polarities at controllable rates.

Keywords: Dendrigraft polymers; Dendritic micelles; Solubilization

1. Introduction

Polymers containing covalently bonded hydrophilic and hydrophobic chain segments can self-associate into micelles when dissolved in solvents selective for one of the components. This phenomenon has sparked interest in the application of amphiphilic copolymers in different areas including the fabrication of nanoscale assemblies, the aqueous solubilization of hydrophobic compounds, drug delivery, and environmental remediation [1]. Most solubilization studies have used block copolymers, and it has been established that the solubilization behavior is affected by the composition, molecular weight, and concentration of the copolymer, as well as by solvent composition [2,19]. Because solubilization by block copolymers is based on their ability to form micelles via dynamic equilibrium with unassociated species at concentrations above the critical micelle concentration (CMC), solvency conditions have a strong influence on micelle structure and stability. This limits their usefulness as drug delivery and environmental decontamination agents.

Certain amphiphilic copolymer architectures incorporating a branched component, such as the dendritic-linear block copolymer hybrids, have been shown to form multimolecular micelles analogous to block copolymer micelles by self-assembly [3]. In contrast, amphiphilic dendritic polymers with polar groups on their periphery often behave like unimolecular (non-associated) micelles, maintaining their overall shape irrespective of their environment, and displaying no CMC. Because of these remarkable characteristics the past decade has witnessed a surge of interest in the synthesis and characterization of dendritic polymer micelles, particularly in relation to biomedical applications [4]. These nanoscale molecules, characterized by the presence of monomeric branches (dendrimers and hyperbranched polymers) or polymeric branches

* Corresponding author. Tel.: +1 519 888 4567; fax: +1 519 746 0435.
E-mail address: gauthier@uwaterloo.ca (M. Gauthier).

0032-3861/$ - see front matter © 2008 Elsevier Ltd. All rights reserved.
doi:10.1016/j.polymer.2008.01.016

(dendrigraft polymers) emanating from a central core, may potentially be useful to replace block copolymers in applications such as drug delivery systems, microencapsulation, and catalysis.

One drawback of dendrimers and hyperbranched polymers is their small size (1–10 nm), making them less efficient than block copolymer micelles in certain applications. For example, micelles and liposomes with a size in the 100–200 nm range have a long blood circulation time and are able to penetrate tumor cells by different mechanisms, and are therefore potentially more useful than dendrimers and hyperbranched polymers to target certain tissues with drugs [5].

Arborescent polymers are a family of dendrigraft polymers obtained from successive grafting reactions of polymeric building blocks in a generation-based scheme analogous to dendrimer syntheses [6]. Arborescent polymers have a highly branched architecture, a narrow size distribution ($M_w/M_n < 1.1$), a very high molecular weight ($M_w = 10^4$–10^8), and a hydrodynamic diameter of 10–200 nm attained in only a few reaction cycles. These molecules have the additional advantage that many of their structural parameters could be varied to tailor their micellar properties to meet specific requirements. For example in a good solvent, the degree of swelling of arborescent micelles could be controlled by varying either the branching functionality, the molecular weight of the chains in the core and the corona, or through the generation number. In a previous paper [7] we reported a procedure for the synthesis of arborescent polystyrene (PS) grafted with poly(2-vinylpyridine) (P2VP) segments, using acetyl functionalities as coupling sites on the PS substrates. Dynamic light scattering measurements revealed that while copolymers derived from linear polystyrene associated into micellar superstructure when dissolved in aqueous HCl, copolymers incorporating branched (generations *G*0–*G*2PS) substrates remained unassociated as unimolecular micelles under the same conditions.

In this study, we focus our attention on the aqueous solubilization of polycyclic aromatic hydrocarbons (PAHs; Fig. 1) by PS-*g*-P2VP arborescent unimolecular micelles. This is the first systematic investigation of the solubilization properties of amphiphilic dendrigraft copolymers for a range of hydrophobic probes as a function of copolymer structure. The probes were selected not only to clarify the influence of probe hydrophobicity, size, symmetry, and physical state on micellar loading and the rate of solubilization, but also to determine the location of the probes within the micelles. While the arborescent copolymers used are not biocompatible, they serve as model compounds to demonstrate the ability to control the solubilization characteristics (capacity and kinetics) of these micelles through structural variations. The understanding gained will be useful in tailoring the properties of these and other biocompatible dendrigraft polymers for controlled drug delivery applications.

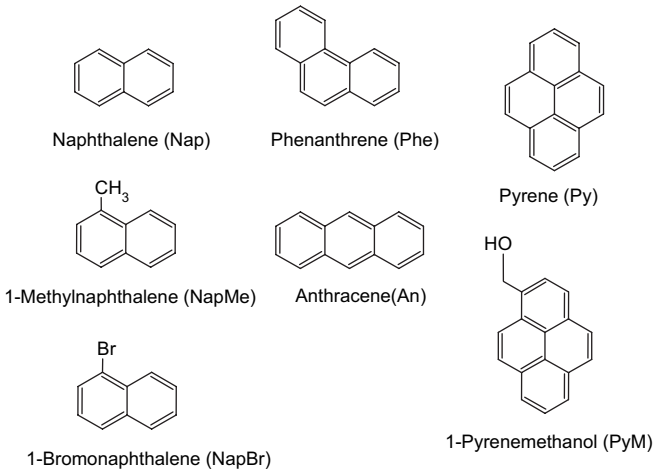

Fig. 1. Structure of polycyclic aromatic hydrocarbons used.

2. Experimental

2.1. Sample preparation

Anthracene (An, 99+%), 1-bromonaphthalene (NapBr, 99%), 1-methylnaphthalene (NapMe, 99%), naphthalene (Nap, 99+%), phenanthrene (Phe, 99+%), pyrene (Py, 99%), and 1-pyrenemethanol (PyM, 98%) were obtained from Aldrich. Py and PyM were recrystallized twice from ethanol; NapBr and NapMe were distilled under reduced pressure. An, Nap, and Phe were used as-received. Milli-Q water was used to prepare all samples. The arborescent PS-*g*-P2VP copolymers used were synthesized by anionic grafting of P2VP chains onto acetylated polystyrene substrates of different generations [7]. All samples had a narrow molecular weight distribution ($M_w/M_n < 1.1$) and a polystyrene weight fraction of at most 20%. Micellar solutions (1.5 mg/mL) were prepared by dissolving 75 mg of arborescent copolymer in 50 mL of 0.05 M HCl. After complete dissolution, 75 mg of PAH was added to each solution. The samples were left to equilibrate in the dark without stirring, to avoid breakup of the crystals complicating their removal by filtration. Micellar copolymer solutions (1.5 mg/mL) without PAH were also prepared to serve as blank solutions for the UV measurements.

2.2. Fluorescence and UV measurements

Aliquots (3 mL) of the micellar solutions were withdrawn at predetermined time intervals and filtered using a 0.22 μm pore size mixed cellulose ester (Millipore AAWP) membrane filter. Hellma quartz cells (1.0 × 1.0 cm^2) were used for the fluorescence and UV measurements. The UV measurements were carried out on a Hewlett–Packard 8452A Diode Array Spectrophotometer after dilution of the samples to obtain absorbance readings below 1.5. Normalized absorbance values were calculated to report the results by multiplying the actual absorbance reading by the dilution factor necessary to bring the absorbance below 1.5. Hydrophobic probe uptake was monitored until the readings became constant. Steady-state fluorescence studies were carried out using a Photon Technology International LS-100 spectrometer with a pulsed xenon flash lamp light source. The samples were deoxygenated for 20 min by bubbling with

nitrogen. Dilution was necessary in most cases to reduce the optical density of the solutions to 0.3 or less before the fluorescence measurements, to minimize inner filter effects. For both Py and PyM fluorescence emission spectra the excitation wavelength was set at 344 nm. To avoid inconsistencies due to lamp intensity variations, the fluorescence intensity of a Py standard was measured to allow the normalization of each spectrum.

The solubility of PyM and Py in 0.05 M HCl was estimated from a calibration curve obtained in pure water from fluorescence measurements following the protocol of Kwon et al. [8]. A stock solution of each compound was prepared by first dissolving 2.40 mg of PAH in HPLC grade acetone, after which acetone was evaporated. Milli-Q water (250 mL) was added and the solution was stirred overnight for equilibration. The solution was then filtered through a 0.22 μm mixed cellulose ester filter to remove residual crystals. The concentration of the saturated aqueous solution was confirmed by UV absorption measurements. Sample solutions of different concentrations were then prepared by dilution of stock solution aliquots with Milli-Q water. Steady-state measurements were carried out on the solutions and the intensity of the emission peak at 373 nm (I_1) was used to establish calibration curves for both PyM and Py.

3. Results and discussion

It has been shown that amphiphilic dendrimers are capable of greatly enhancing the aqueous solubility of hydrophobic molecules [9]. Encapsulation by these unimolecular micelles may rely on physical entrapment of the guest molecules, the formation of non-covalent interactions between the guest molecules and the carrier, or hydrophobic interactions [4f]. For dendrimers the absorption capacity is simply a function of the number of internal cavities available for entrapment, which depends on the generation number. The situation becomes more complex when dealing with charged micellar systems [10]. For example block copolymer micelles with a polyelectrolyte shell have a larger size than non-ionic copolymer micelles, despite their smaller aggregation number. The micellar properties of such systems are strongly influenced by the nature of the corona that, in turn, is sensitive to the pH and ionic strength of the solution [11]. Arborescent PS-*g*-P2VP copolymers have been found to expand upon ionization with HCl, in analogy to polyelectrolyte micelles [12]. In the present study we examined the solubilization of a series of PAHs by arborescent PS-*g*-P2VP copolymers in acidified aqueous solutions. The influence of probe size, symmetry, and substituents on the solubilization process has been examined. Two fundamental parameters used for this purpose are the solubilization capacity κ^G (expressed as mg probe/g micelle) and the partition coefficient K_w [13].

$$\kappa^G = \frac{S^G_{tot} - S^G_s}{C^G_{mic} - CMC^G} \quad (1)$$

$$K_w = \frac{S_{mic}}{S_s} \quad (2)$$

where S^G_{tot} is the total concentration of the probe in the micellar solution (mg/mL), S^G_s is the concentration of the probe in the solvent (mg/mL), S_{mic} is the number of moles of probe solubilized per gram of micelles, and S_s is the number of moles of probe dissolved per gram of solvent. In the present case the micelle concentration C^G_{mic} (g/mL) is set to the copolymer concentration, since the critical micelle concentration CMC^G (g/mL) is zero for unimolecular micelles. The architecture of some copolymers of the type used in the study is compared in Fig. 2. These copolymers were obtained from successive anionic grafting reactions as described previously [7]. The characteristics of the copolymers used are summarized in Table 1. The nomenclature used for arborescent copolymers identifies their composition and structure. For example, *G*1PS–P2VP5–13 refers to a graft copolymer synthesized from a *G*1 polystyrene core ($M_w \approx 5000$ linear PS grafted twice with $M_w \approx 5000$ PS side chains), coupled with $M_w \approx 5000$ P2VP side chains in a third grafting reaction, with a PS content of 13% by weight.

The branching functionality of the core and the whole molecule, defined as the number of side chains added in the last grafting reaction, was calculated from the equation:

$$f_w = \frac{M_w(G) - M_w(G-1)}{M^{br}_w} \quad (3)$$

where $M_w(G)$, $M_w(G-1)$ and M^{br}_w are the absolute weight-average molecular weights for graft polymers of generation G, of the preceding generation, and of the side chains, respectively, and obtained either from size exclusion chromatography using a multi-angle laser light scattering detector (SEC-MALLS) or from batch-wise light scattering measurements.

3.1. Equilibrium probe uptake

One important parameter affecting probe uptake in solubilization experiments with block copolymers is their hydrophobic component content. For example, Hurter and Hatton [2b] found that the partition coefficient for naphthalene in solutions of Pluronic® copolymers varied as a function of the poly(ethylene oxide)–poly(propylene oxide) ratio. They further determined that for micelles obtained from copolymers of identical composition, copolymers with a higher molecular weight had higher solubilization capacities and partition coefficients. Cao et al. [2a] compared absorption capacity values for their

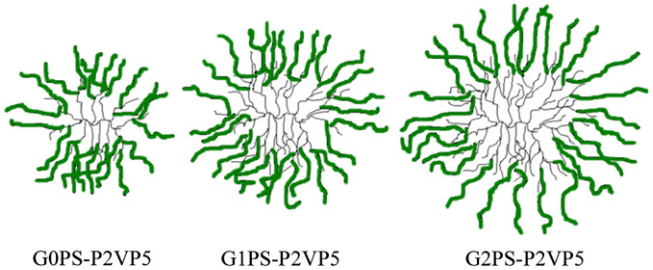

Fig. 2. Structure of arborescent PS-*g*-P2VP5 copolymers of different generations.

Table 1
Characteristics of arborescent PS-*g*-P2VP copolymers used

Sample	P2VP side chains		Graft copolymers				
	M_w [a]	M_w/M_n [a]	M_w [a]	M_w/M_n [a]	$f_{w(core)}$	$f_{w(copol)}$	Wt% PS [b]
*G*0PS–P2VP5–12	5100	1.06	4.7×10^5	1.08	11	82	12
*G*1PS–P2VP5–13	5200	1.08	3.7×10^6	1.07	84	630	13
*G*1PS–P2VP5–20	5200	1.09	2.4×10^6	1.09	84	370	20
*G*2PS–P2VP5–18	5300	1.07	2.2×10^7	NA	690	3400	18
*G*0PS–P2VP30–3	32 000	1.07	2.2×10^6	1.07	11	67	3
*G*1PS–P2VP30–4	32 000	1.07	1.1×10^7	1.08	84	330	4

[a] Absolute values determined from SEC-MALLS or laser light scattering measurements; *G*2PS–P2VP5–18 retained on column in SEC analysis.
[b] PS content determined by ^{1}H NMR spectroscopy.

poly(methacrylic acid)-*block*-polystyrene-*block*-poly(methacrylic acid) copolymer micelles to those reported by Dowling and Thomas [14] for micelles obtained from acrylamide–styrene copolymers with a "blocky" microstructure. The high pyrene absorption capacity ($\kappa^G = 32$ mg/g) of the methacrylic acid micelles as compared to the acrylamide micelles of $\kappa^G = 1$ mg/g was attributed to their higher polystyrene content. More recent studies [9] have shown that pyrene uptake by dendrimers is a direct function of generation number, and therefore molecular size. It was argued that higher generation dendrimers were able to solubilize more pyrene specifically because they contained more microcavities for encapsulation.

The solubility of PyM in aqueous solutions was strongly enhanced by arborescent copolymers containing either short (P2VP5) or long (P2VP30) poly(2-vinylpyridine) side chains, but the effect was more pronounced for the copolymers with shorter polyelectrolyte chains. The influence of copolymer structure and composition on solubilization is illustrated in Fig. 3 for PyM with UV absorption spectra obtained for copolymer solutions (1.5 mg/mL) equilibrated with the probe. Similar measurements for 0.05 M HCl solutions saturated with PyM in the absence of copolymer yielded a barely detectable signal on the UV spectrometer used. The UV absorption spectra in Fig. 3 indicate that PyM micellar loading for arborescent PS–P2VP copolymers correlates approximately with the PS content of the micelles, as solubilization increases with the PS content of the copolymers. Based on the above discussion regarding the influence of dendrimer size, micelles of *G*1PS–P2VP5–13, with a PS content comparable to *G*0PS–P2VP5–12 but larger in size, would be expected to have a higher solubilization capacity. The opposite result was observed experimentally, as the UV absorbance for *G*0PS–P2VP5–12 in Fig. 3 is significantly higher than for *G*1PS–P2VP5–13. One important characteristic of arborescent polymers is their increasing segmental density for higher generations, because of their increasingly hard sphere-like character [15]. This is partly a consequence of the larger number of branching points in *G*1PS–P2VP5–13 ($f_w = 630$) than in *G*0PS–P2VP5–12 ($f_w = 82$). The solubilization of hydrophobic probes in the non-polar PS core may become more difficult due to increased segmental density in copolymers with a higher branching functionality f_w. On that basis, lower generation arborescent copolymers may be able to solubilize a larger amount of hydrophobic guest compounds than higher generation copolymers of similar composition.

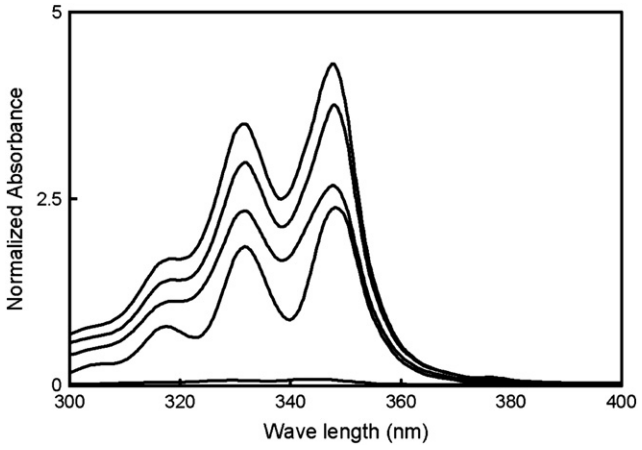

Fig. 3. UV equilibrium absorption spectra for PyM solubilized by arborescent copolymer samples. The curves, from top to bottom, are for *G*1PS–P2VP5–20, *G*2PS–P2VP5–18, *G*0PS–P2VP5–12, *G*1PS–P2VP5–13, and *G*0PS–P2VP30–3.

For copolymers with long branches (P2VP30), solubility enhancement for PyM was minimal (Fig. 3, bottom curve). Though the longer P2VP chains of the P2VP30 copolymers might have hindered the diffusion of PyM molecules to the PS core, the much lower polystyrene content of the P2VP30 copolymers is likely the main reason for lower PyM uptake. Because of their very low absorption capacity, investigations of copolymers based on P2VP30 side chains were more limited.

3.2. Micellar uptake kinetics

The kinetics of the absorption process were investigated by monitoring PyM uptake as a function of time. Equilibration was assumed when a plateau was reached in the absorbance versus time plot (Fig. 4). Composition and branching functionality have a significant influence on the equilibration time of the P2VP5 copolymer samples: copolymers with higher PS contents and f_w have longer equilibration times (25–35 days) than copolymers with lower PS contents and f_w (8–20 days). Quantitative information on the rate of solubilization was obtained using the first-order kinetic equation [16]:

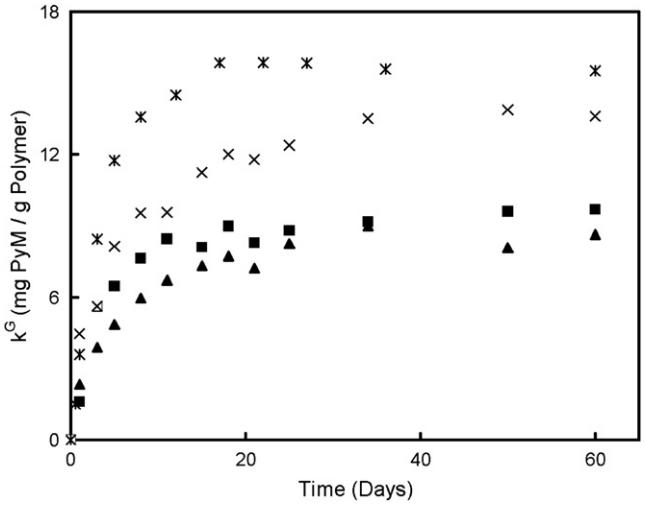

Fig. 4. Time dependence of PyM uptake by arborescent micelles: (■) *G*0PS–P2VP5–12; (▲) *G*1PS–P2VP5–13; (✱) *G*1PS–P2VP5–20; × *G*2PS–P2VP5–18.

$$[\mathrm{PyM}]_t = [\mathrm{PyM}]_{\mathrm{eq}}(1 - \exp(-kt)) \quad (4)$$

to fit our data, where $[\mathrm{PyM}]_{\mathrm{eq}}$ is the equilibrium concentration of PyM in the micelles, and $[\mathrm{PyM}]_t$ is the concentration of PyM in the micelles at time t. With this expression, it was possible to quantify the uptake rate in terms of the rate constant k.

Fig. 5 is a plot of $\ln([\mathrm{PyM}]_{\mathrm{eq}} - [\mathrm{PyM}]_t)$ versus time, corresponding to the logarithmic form of Eq. (4). The rate of PyM uptake depends on both branching functionality and copolymer composition, as seen from the different rate constants (slopes) observed for the copolymers. The lower solubilization rates observed for higher generation arborescent copolymers are attributed to the higher branching functionality of the micelles making it more difficult for the probe to diffuse inside, as outlined above. If this hypothesis is valid, decreasing the branching functionality of the copolymer micelles should enhance the uptake rate. The branching functionality of a copolymer sample was decreased by lowering the acetylation level of the *G*1PS substrate used in its synthesis. Samples

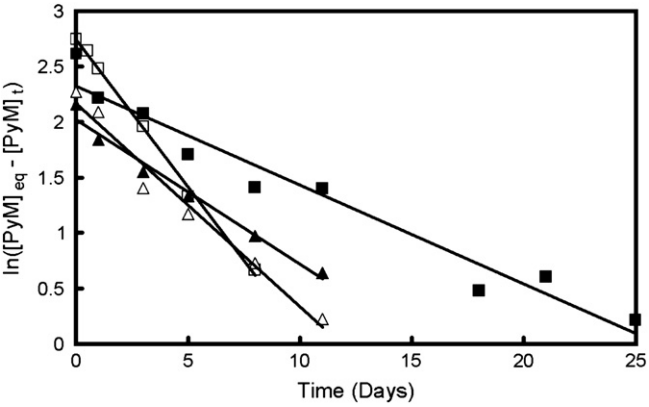

Fig. 5. Analysis of micellar uptake kinetics. The following rate constants were obtained: (△) *G*0PS–P2VP5–12, $k = (0.18 \pm 0.01)\ \mathrm{d}^{-1}$; (▲) *G*1PS–P2VP5–13, $k = (0.13 \pm 0.01)\ \mathrm{d}^{-1}$; (□) *G*1PS–P2VP5–20, $k = (0.266 \pm 0.006)\ \mathrm{d}^{-1}$; (■) *G*2PS–P2VP5–18, $k = (0.089 \pm 0.007)\ \mathrm{d}^{-1}$.

*G*1PS–P2VP5–13 and *G*1PS–P2VP5–20 were synthesized from the same polystyrene core, using acetyl group (coupling site) contents of 25 and 8 mol%, respectively. This explains the lower branching functionality and higher PS content obtained for *G*1PS–P2VP5–20. As can be seen from their respective rate plots (Fig. 5), *G*1PS–P2VP5–20 has a significantly higher rate constant ($k = 0.27\ \mathrm{d}^{-1}$) than *G*1PS–P2VP–13 ($k = 0.13\ \mathrm{d}^{-1}$). The range of solubilization rate constants obtained, 0.09–0.27 d^{-1} for the different samples, suggests that it is possible to control the rate at which the hydrophobes are solubilized in the micelles with proper design of the copolymer architecture.

3.3. Determination of partition coefficient and solubilization capacity

The partition of a hydrophobic probe between the bulk aqueous phase and the micelles can be characterized by the partition coefficient at equilibrium, K_{w}, and the solubilization capacity, κ^{G}. Partition experiments were conducted to determine the influence of polymer as well as probe structure on K_{w} and κ^{G}.

Preliminary measurements to determine the solubility of PyM in acidified water (0.05 M HCl) showed that it was about five times lower than in neutral water. Consequently, solubility limits reported for the probes in the literature could not be used for S_{s} in Eq. (2), but rather had to be determined under the conditions described in Section 2. The aqueous solubility of PyM and Py estimated by fluorescence is 1.8×10^{-6} and 9.8×10^{-8} M for PyM and Py, respectively. The solubility of Nap (9.3×10^{-5} M), 1-NapBr (2.6×10^{-5} M), NapMe (6.4×10^{-5} M) and Phe (4.9×10^{-5} M) in aqueous 0.05 M HCl was sufficiently high to determine their concentration from UV absorption measurements. Because of instrumental limitations, the solubility of An in 0.05 M HCl could not be determined. A literature value (2.8×10^{-7} M) [17] for the solubility in pure water was used in this case, so the K_{w} values determined for An are likely underestimated. Because of important differences in the behavior of highly hydrophobic (Py, PyM, An, Phe) and less hydrophobic (Nap, NapBr, NapMe) probes, the results obtained for each series of compounds will be discussed separately.

3.4. Solubilization of highly hydrophobic probes

From Table 2 it was found that the partition coefficient for PyM increases with the PS content of the copolymers, with values ranging from 0.9 to 1.7×10^5. For Py, a more hydrophobic probe than PyM, the partition coefficient is even higher, ranging from 0.3 to 1.2×10^6. An and Phe also have higher K_{w} values for copolymers with a higher PS content. Similar trends have been observed in other studies using block copolymer micelles [2,8,18,19].

The octanol–water partition coefficient (K_{ow}), as a measure of probe hydrophobicity, and the boiling point (bp) of small molecule hydrophobes have been correlated successfully with K_{w} values for block copolymer micelles in the past

Table 2
Partition coefficient K_w for PAHs

Sample	K_w PyM	K_w Py	K_w An	K_w Phe	K_w Nap	K_w NapMe	K_w NapBr
*G*0PS–P2VP5–12	9.6×10^4	3.7×10^5	1.2×10^5	1.7×10^5	8.7×10^2	2.2×10^4	5.0×10^3
*G*1PS–P2VP5–13	8.9×10^4	2.8×10^5	8.1×10^4	1.8×10^5	9.5×10^2	2.3×10^4	9.7×10^3
*G*1PS–P2VP5–20	1.7×10^5	1.2×10^6				3.1×10^4	
*G*2PS–P2VP5–18	1.5×10^5	7.0×10^5	3.1×10^5	4.1×10^5	2.1×10^3	2.9×10^4	1.5×10^4

Abbreviations used: PyM, 1-pyrenemethanol; Py, pyrene; An, anthracene; Phe, phenanthrene; Nap, naphthalene; NapMe, 1-methylnaphthalene; NapBr, 1-bromonaphthalene.

[1b,2b,20]. These properties are reported in Table 3 for the probes used in the present study. The partition coefficients reported in Table 2 indeed increase with the octanol–water partition coefficients reported in Table 3 within the series PyM < Phe ≈ An < Py as expected, as the solubility of the probes in water decreases with increasing hydrophobicity. Almgren et al. [20] have successfully correlated the partition coefficient for a series of arenes in alkyltrimethylammonium bromide and sodium alkyl sulfate micelles to their boiling points. For both types of ionic micelles, a linear relationship was obtained between the boiling point and the partition coefficient of the arenes. The correlation is likewise successful in terms of boiling points of the probes in the limited series Phe = An < Py.

In contrast, no clear trends are observed when trying to correlate the solubilization capacity κ^G (Table 4) to either K_{ow} values or boiling points. For example, An and Phe are tricyclic isomers of very similar hydrophobicity, as indicated by their log K_{ow} values of 4.56 and 4.52, respectively (Table 3). These two compounds might therefore be expected to have similar κ^G values. While K_w is similar for both molecules, the solubilization capacity for Phe is much higher than for An. Correlation of κ^G with the boiling point of the probes used is likewise unsuccessful. Molecular size arguments have been used in the past to explain the decreasing solubilization capacity of Pluronic® block copolymer micelles for hydrophobes in the series Nap, Phe, Py [2b]. As the number of benzene rings per molecule is increased, solubilization should become energetically more difficult because of the larger volume of the solute molecules. On that basis, higher κ^G values would be expected for the solubilization of An and Phe by arborescent micelles than for Py and PyM. Unfortunately the κ^G values observed for arborescent copolymers are larger for Py than for An, and larger for PyM than for An and Phe. The lack of trends in the current investigation suggests that molecular size, hydrophobicity, and solute–solute interactions are not dominant factors determining (at least individually) the solubilization capacity of arborescent copolymer micelles.

Table 3
Physical properties of PAHs [17]

	log K_{ow}	Bp (°C)
Naphthalene	3.34	217.9
1-Methylnaphthalene	3.87	244.7
1-Bromonaphthalene	4.35	281
Anthracene	4.56	339.9
Phenanthrene	4.52	340
Pyrene	5.08	404
1-Pyrenemethanol	3.99	dec

3.5. Solubilization of naphthalene and derivatives

Comparison of the K_w (Table 2) and κ^G (Table 4) values obtained for the different copolymers reveals significant differences in behavior for Nap and its derivatives relative to the larger probes. Nap is the least hydrophobic of all seven probes investigated, and indeed it has the lowest overall K_w values in the series. NapMe, with the second lowest log K_{ow} in the series (albeit close to PyM), ranks third for K_w, behind NapBr. Finally NapBr, with the fourth lowest log K_{ow} value, ranks second lowest in terms of K_w.

A striking difference is observed for Nap and its derivatives in terms of solubilization capacities (Table 4): the κ^G values for NapMe and NapBr, in particular, are much higher than for the other probes. The influence of branching functionality and side chain molecular weight on the physical properties of arborescent polystyrenes has been the object of a number of investigations [21]. Arborescent polystyrene molecules resemble nanonetworks in which they swell in good solvents. Once it is inside the micelles, a liquid hydrophobic probe could behave like a solvent and swell the core to some extent. Naphthalene, NapMe, and NapBr were investigated as probes of lower hydrophobicity than the tri- and tetracyclic PAHs discussed so far. Two of these (NapMe and NapBr) are liquids. It may be tempting to attribute the much higher κ^G values observed for these compounds solely to swelling of the PS micelle cores by the liquid probes. In the following discussion, it will be demonstrated that while core swelling may be of significance, it is likely not the only reason for the higher sorption of the naphthalene probes.

3.6. Location of the probes in the micelles

It has been suggested [13] that the morphology of polymeric micelles includes three regions: the hydrophobic core, the hydrophilic shell (corona), and the so-called palisade, which is the interfacial region between the core and the shell. For a more complete understanding of a micellar system, it is worthwhile to determine where the molecular solute is located

Table 4
Solubilization capacity κ^G (mg probe/g polymer) for PAHs

Sample	κ^G PyM	κ^G Py	κ^G An	κ^G Phe	κ^G Nap	κ^G NapMe	κ^G NapBr
*G*0PS–P2VP5–12	8.7	2.5	0.3	4.9	10	35	27
*G*1PS–P2VP5–13	8.1	1.8	0.2	5.5	11	39	53
*G*2PS–P2VP5–18	14	4.6	0.8	12	25	99	81
*G*1PS–P2VP5–20	15	8.0				120	

inside the micelles. Depending on the relative hydrophobicity of a probe and the copolymer components, a probe can be located in one or more of the three regions mentioned. Highly hydrophobic solutes are typically solubilized in the micellar core, while semipolar and polar solutes can be solubilized in the palisade and/or the corona. It is well established that increasing the hydrophobic phase content of micellar systems greatly enhances the solubilization capacity and partition coefficient for Py, a highly hydrophobic probe preferentially solubilized in the core [2a,b,14]. In contrast, the solubilization of semipolar solutes remains almost unaffected by the hydrophobic phase content [13,22]. In such situations, the semipolar solutes are said to be associated with either the palisade or the hydrophilic corona. For relatively polar solutes, solubilization may even decrease with increasing hydrophobic phase content, due to preferential sorption in the corona [23].

A plot of the partition coefficient K_w versus PS weight fraction is used in Fig. 6 to compare the behavior of three of the probes used (Py, PyM, and NapMe). The partition coefficient for Py increases sharply as the PS content of the copolymer increases, in analogy to other micellar systems. This suggests that Py is located predominantly in the core of the micelles. In contrast, the relative increase in K_w is less significant for PyM and minimal for NapMe. The insensitivity of K_w to composition for PyM and NapMe could be explained by preferential partition of these more polar compounds to the palisade and/or corona regions of the micelles.

If the corona region contributes significantly to the solubilization process, copolymers in the P2VP30 series, with a very low PS content, should have a higher solubilization capacity for the polar probes (Nap and derivatives) than for the hydrophobic probes. For both *G*0PS–P2VP30–3 and *G*1PS–P2VP30–4, $\kappa^G = 11$ mg/g was determined using Nap as probe. The same copolymers yielded $\kappa^G = 17$ and 21 mg/g, respectively, for NapBr. In comparison, $\kappa^G = 0.08$ mg/g for PyM in *G*0PS–P2VP30–3, and the amount of Py solubilized by the same compound was too low to be detected. On the basis of these results, the high κ^G values observed for the Nap derivatives are attributable at least in part to non-selective sorption of the probes, beyond the core swelling effect already discussed: a significant portion of these compounds must be located inside the corona and/or palisade regions of the P2VP-rich micelles, rather than preferentially in the core as in the case of pyrene. The low sorption capacity observed for PyM relative to the naphthalene derivatives is consistent with its location in a restricted volume outside the core, i.e. the palisade region.

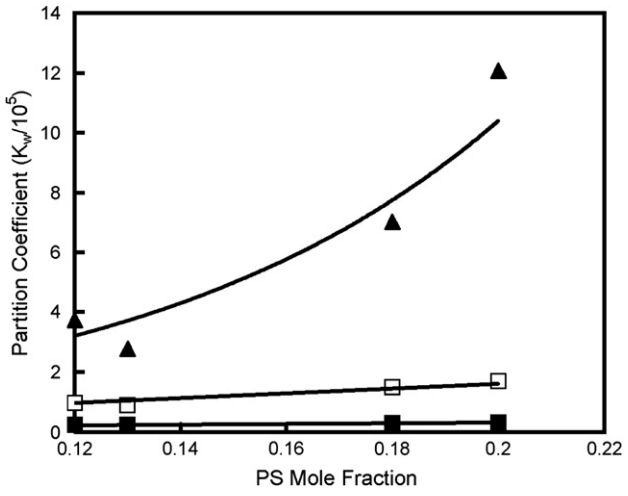

Fig. 6. Composition dependence of partition coefficient for (▲) Py, (□) PyM, and (■) NapMe.

3.7. Additional evidence in support of selective sorption

The intensity of fluorescence emission observed was compared for PyM in 0.05 M HCl, in the presence of linear P2VP, and with the arborescent copolymer micelles. The ratio of intensities determined for the first vibronic band I_1 (373 nm) of PyM in acidified water, and in acidified solutions of linear P2VP and *G*0PS–P2VP5–12 after attainment of equilibrium conditions was 1:4:75. The large intensity difference observed between linear P2VP and *G*0PS–P2VP5 confirms that the solubility of PyM in ionized P2VP is very low. The fraction of PyM associated strictly with the P2VP shell of arborescent PS–P2VP5 copolymers is therefore considered negligible under the conditions used, and these probes must be located predominantly in the palisade region.

A red shift in the UV absorption spectrum was observed for PyM, as λ_{max} shifted from 342 nm for the P2VP30 copolymers to 348 nm for the P2VP5 copolymers (Fig. 7). A study of PyM [24] has demonstrated that in a hydrophobic environment such as PS, λ_{max} is higher (346 nm) than in polar environments (339 nm for MeOH). Red shifts have also been observed for the fluorescence excitation spectrum of pyrene [3c,18,25] and the UV absorption spectrum of a cyclic disulfide containing pyrene residues [26]. These effects have been linked systematically to the transfer of Py from water to a more hydrophobic environment. The change in λ_{max} observed for PyM in the present study confirms that the small amount of PyM solubilized by the long-branch (P2VP30) copolymers resides mainly in a more hydrophilic (P2VP-rich) environment, corresponding to the P2VP hydrophilic shell. It is interesting to note that the peak at $\lambda_{max} = 342$ nm for the P2VP30 copolymers is somewhat distorted by a shoulder, suggesting a partial contribution to the peak originating from core-solubilized PyM. Considering the lower intensity of the shoulder and the much lower solubilization capacity of the P2VP30 copolymers, however, it is clear that the PyM solubilized by short-branch (P2VP5) copolymers resides predominantly in a more hydrophobic region such as the core and/or the palisade.

Additional evidence for partitioning of the hydrophobic probes within the micelles was obtained from steady-state fluorescence measurements using Py, since it is a widely used polarity-sensitive probe. The intensity ratio for the first vibronic band I_1 (373 nm) to the third vibronic band I_3 (383 nm) undergoes significant changes with solvent polarity, as a result of coupling of the electronic and vibronic states, and can serve to monitor the polarity of the microenvironment surrounding the probe [27]. For *G*2PS–P2VP5–18, an I_1/I_3

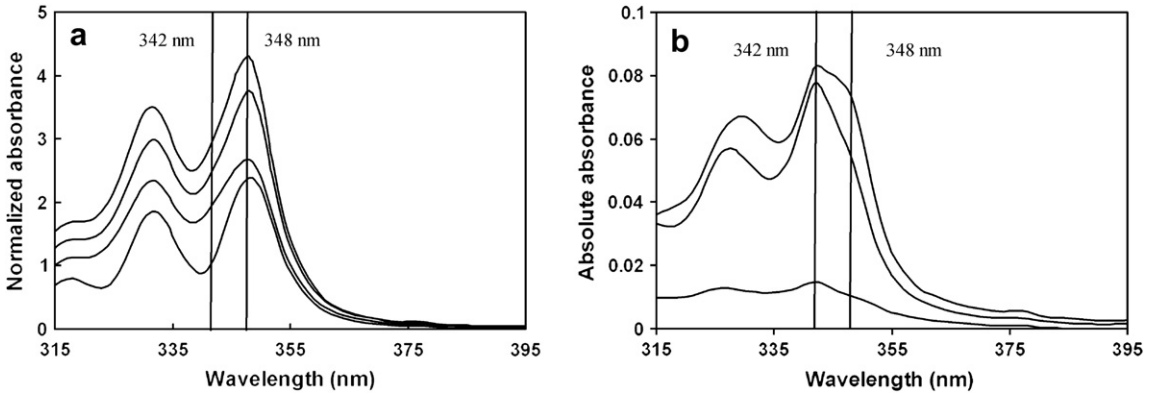

Fig. 7. Red shift of UV absorbance for PyM in (a) P2VP5 and (b) P2VP30 samples. $\lambda_{max} = 342$ nm for P2VP30 samples, 348 nm for P2VP5 samples; an absolute absorbance scale is used for the P2VP30 samples.

value of 1.03 ± 0.01 was obtained, and for *G*1PS–P2VP5–20, the I_1/I_3 value was 0.97 ± 0.03. Literature values for I_1/I_3 in water range from 1.6 to 1.96 [27a,28]. The ratio decreases for increasing microenvironment hydrophobicity, to 0.95 in PS films, for example [18]. The I_1/I_3 ratios obtained for the arborescent copolymers are consistent with the concentration of Py within the PS core of the micelles.

Finally, it is interesting to note the absence of the broad PyM and Py excimer emission peaks for all the PS–P2VP copolymer micelle solutions investigated, even at very high probe uptake. Excimer formation can result from a dynamic process, whereby an electronically excited pyrene diffuses to encounter a pyrene molecule in its ground state, or from a static process involving the excitation of preassociated ground state pyrene molecules. It was suggested that diffusion-controlled excimer formation inside a hydrophobic domain depends on the microviscosity of the micelles [29]. According to this interpretation, the lack of an excimer peak for Py and PyM is consistent with a very dense (collapsed) core structure, making it almost impossible for two closely located probe molecules to diffusionally encounter during the lifetime of the excited molecule. While excimer peaks are absent, the possibility of probe aggregation cannot be excluded. There are reports on the preassociation of pyrene and its derivatives in molecular assemblies [24,30]. In some instances, extensive self-quenching due to the low quantum yield of these aggregates has been reported [30,31]. In such situations the broad peak at 485 nm in the fluorescence emission spectrum, associated with excimer formation, decreases in intensity or even disappears. The peak-to-valley ratio for the UV absorption spectrum of the most intense band of Py derivatives (ca. 348 nm) to that of the adjacent minimum at shorter wavelength (ca. 338 nm) has been linked to preassociation in pyrene-labeled polymers [31]. This method is convenient to detect preassociation when no excimer emission peak is observed. A peak-to-valley ratio greater than 3 indicates the absence of aggregation; the ratio decreases for increasing preassociation. From the absorption spectra of PyM (Fig. 3) and Py (not shown), the peak-to-valley ratio ranges from 1.6 to 2.86 for all micellar solutions, suggesting that some of the probe molecules are aggregated in the ground state.

The preassociation of pyrene-labeled polymers is sometimes accompanied by a hypochromic effect (decrease in molar extinction coefficient) [32]. From Fig. 3 it was found that PyM in *G*1PS–P2VP5–13 has the highest peak-to-valley ratio of $\sim$2.69, and the hypochromic effect is therefore likely to be minimal (least association) for this sample as compared to PyM in the other copolymer solutions. If this is true, the solubilization capacity of *G*1PS–P2VP5–13 may be underestimated, since the same molar extinction coefficient ($35\,900\ mol^{-1}\ cm^{-1}$, $\lambda_{max} = 346$ nm in toluene) was used to analyze all the micellar solutions. This observation has no bearing on the fact that for copolymers of different generations with similar compositions, the lower generation copolymers have a higher solubilization capacity, however. Furthermore, Py had similar peak-to-valley ratios for all copolymer solutions investigated, and the solubilization capacity was greater for *G*0PS–P2VP5–12 than for *G*1PS–P2VP–13.

4. Conclusions

Partitioning of hydrophobic solutes between arborescent polystyrene-*graft*-poly(2-vinylpyridine) unimolecular micelles and water depends on both the structure of the micelles and the nature of the probes. Arborescent copolymers with a high PS content are far better sorbents than samples with a low PS content. The structure of the solute also has a large effect on the partition coefficients and micelle loadings observed. Pyrene has partition coefficients reaching $\sim 10^6$, however, probes with a lower hydrophobicity give higher micelle loadings. The generation number and hydrophobic content of the copolymers have a significant influence on both uptake capacity and kinetics. For samples in the P2VP5 series, the partition coefficient increases rapidly with the PS mole fraction of the copolymers for highly hydrophobic probes, while only a minor increase is observed for probes of lower hydrophobicity. For copolymers of different generations with similar PS contents, however, the solubilization capacity is higher for the lower generation copolymers. Copolymers with a higher branching functionality are also characterized by lower probe solubilization rates. These results are consistent with the segmental

density of arborescent polymer molecules increasing for higher generations, as determined in previous studies.

Acknowledgements

We are grateful for the financial support of the Natural Sciences and Engineering Research Council of Canada (NSERC) and the International Council for Canadian Studies (ICCS) for this work. We are also indebted to Prof. Jean Duhamel for useful discussions and for providing access to the fluorescence equipment.

References

[1] (a) Yokoyama M, Kwon GS, Okano T, Sakurai Y, Seto T, Kataoka K. Bioconjugate Chem 1992;3:295–301;
(b) Haulbrook WR, Feerer JL, Hatton TA, Tester JW. Environ Sci Technol 1993;27:2783–8;
(c) Quintana JR, Salazar RA, Katime I. Macromolecules 1994;27:665–8;
(d) Kwon GS, Okano T. Adv Drug Delivery Rev 1996;21:107–16;
(e) Richardson MF, Armentrout RS, McCormick CL. J Appl Polym Sci 1999;74:2290–300;
(f) van Domeselaar GH, Kwon GS, Andrew LC, Wishart DS. Colloids Surf B Biointerfaces 2003;30:323–34;
(g) Glass R, Arnold M, Blümmel J, Küller A, Möller M, Spatz JP. Adv Funct Mater 2003;13:569–75.

[2] (a) Cao T, Munk P, Ramireddy C, Tuzar Z, Webber SE. Macromolecules 1991;24:6300–5;
(b) Hurter PN, Hatton TA; Langmuir 1992;8:1291–9;
(c) Gadelle F, Koros WJ, Schechter RS. Macromolecules 1995;28:4883–92.

[3] (a) Gitsov I, Fréchet JMJ. Macromolecules 1993;26:6536–46;
(b) Fréchet JMJ, Gitsov I. Macromol Symp 1995;98:441–65;
(c) Chang Y, Kwon YC, Lee SC, Kim C. Macromolecules 2000;33:4496–500;
(d) Gitsov I, Lambrych KR, Remnant VA, Pracitto R. J Polym Sci Part A Polym Chem 2000;38:2711–27;
(e) Chang Y, Kim C. J Polym Sci Part A Polym Chem 2001;39:918–26;
(f) Gitsov I. In: Newkome GR, editor. Linear-dendritic block copolymers. Synthesis and characterization. Advances in dendritic macromolecules, vol. 5. Amsterdam: Elsevier; 2002 [chapter 2].

[4] (a) Newkome GR, Yao Z, Baker GR, Gupta VK. J Org Chem 1985;50:2003–4;
(b) Hawker CJ, Wooley KL, Fréchet JMJ. J Chem Soc Perkin Trans 1 1993:1287–97;
(c) Fréchet JMJ. Science 1994;263:1710–5;
(d) Stevelmans S, van Hest JCM, Jansen JFGA, van Boxtel DAFJ, de Brabander-van den Berg EMM, Meijer EW. J Am Chem Soc 1996;118:7398–9;
(e) Twyman LJ, Beezer AE, Esfand R, Hardy MJ, Mitchell JC. Tetrahedron Lett 1999;40:1743–6;
(f) Liu M, Fréchet JMJ. Pharm Sci Technol Today 1999;2:393–401;
(g) de Groot D, de Waal BFM, Reek JNH, Schenning APHJ, Kamer PCJ, Meijer EW, et al. J Am Chem Soc 2001;123:8453–8;
(h) Dykes GM. J Chem Technol Biotechnol 2001;76:903–18;
(i) Turro NJ, Chen W, Ottaviani MF. Characterization of dendrimer structures by spectroscopic techniques. In: Fréchet JMJ, Tomalia DA, editors. Dendrimers and other dendritic polymers. West Sussex: Wiley; 2001 [chapter 13];
(j) Newkome GR, Moorefield CN, Vögtle F. Dendrimers and dendrons: concepts, syntheses, applications. New York: Wiley-VCH; 2001;
(k) Weener JW, Baars MWPL, Meijer EW. Some unique features of dendrimers based upon self-assembly and host–guest properties. In: Fréchet JMJ, Tomalia DA, editors. Dendrimers and other dendritic polymers. West Sussex: Wiley; 2001 [chapter 16];
(l) Beezer AE, King ASH, Martin IK, Mitchel JC, Twyman LJ, Wain CF. Tetrahedron 2003;59:3873–80;
(m) Niwa M, Higashizaki T, Higashi N. Tetrahedron 2003;59:4011–5;
(n) Boas U, Christensen JB, Heegaard PMH. Dendrimers in medicine and biotechnology: new molecular tools. Cambridge: Royal Society of Chemistry; 2006.

[5] (a) Kwon G, Suwa S, Yokoyama M, Okano T, Sakurai Y, Kataoka K. J Controlled Release 1994;29:17–23;
(b) Yuan F, Dellian M, Fukumura D, Leunig M, Berk DA, Torchilin VP, et al. Cancer Res 1995;55:3752–6;
(c) Kim SY, Shin IG, Lee YM, Cho CS, Sung YK. J Controlled Release 1998;51:13–22;
(d) Kong G, Braun RD, Dewhirst MW. Cancer Res 2000;60:4440–5;
(e) Ducan R, Izzo L. Adv Drug Delivery Rev 2005;57:2215–37.

[6] For a recent review on the synthesis and properties of arborescent and other dendrigraft polymers, see: Teertstra SJ, Gauthier M Prog Polym Sci 2004;29:277–327.

[7] Gauthier M, Li J, Dockendorff J. Macromolecules 2003;36:2642–8.

[8] Kwon GS, Naito M, Kataoka K, Yokoyama M, Sakurai Y, Okano T. Colloids Surf B Biointerfaces 1994;2:429–34.

[9] (a) Pistolis G, Malliaris A, Paleos CM, Tsiourvas D. Langmuir 1997;13:5870–5;
(b) Liu M, Kono K, Fréchet JMJ. J Controlled Release 2000;65:121–31.

[10] Phoon CL, Higgins JS, Burchard W, Peiffer DG. Macromol Rep 1992;A29(Suppl. 2):179–88.

[11] Astafieva I, Zhong XF, Eisenberg A. Macromolecules 1993;26:7339–52.

[12] Kee RA, Gauthier M. Macromolecules 2002;35:6526–32.

[13] Yalkowsky SH. Solubility and solubilization in aqueous media. New York: Oxford University Press; 1999 [chapter 7].

[14] Dowling KC, Thomas JK. Macromolecules 1990;23:1059–64.

[15] (a) Choi S, Briber RM, Bauer BJ, Topp A, Gauthier M, Tichagwa L. Macromolecules 1999;32:7879–86;
(b) Choi S, Briber RM, Bauer BJ, Liu DW, Gauthier M. Macromolecules 2000;33:6495–501.

[16] Liu G, Zhou J. Macromolecules 2003;36:5279–84.

[17] Mackay D, Shiu WY, Ma KC. Illustrated handbook of physical–chemical properties and environmental fate for organic chemicals. Boca Raton: Lewis; 1992.

[18] Wilhelm M, Zhao CL, Wang Y, Xu R, Winnik MA, Mura JL, et al. Macromolecules 1991;24:1033–40.

[19] Zhao J, Allen C, Eisenberg A. Macromolecules 1997;30:7143–50.

[20] Almgren M, Grieser F, Thomas JK. J Am Chem Soc 1979;101:279–91.

[21] (a) Gauthier M, Li W, Tichagwa L. Polymer 1994;38:6363–70;
(b) Sheiko S, Gauthier M, Möller M. Macromolecules 1997;30:2343–9;
(c) Hempenius MA, Zoetelief WF, Gauthier M, Möller M. Macromolecules 1998;31:2299–304.

[22] Ismail AA, Gouda MW, Motawi MM. J Pharm Sci 1970;59:220–4.

[23] Alkahmis KA, Allaboun H, Al-Momami WY. J Pharm Sci 2003;92:839–46.

[24] Hrdlovič P, Lukáč I. J Photochem Photobiol A Chem 2000;133:73–82.

[25] Nah JW, Jeong YI, Cho CS. Bull Korean Chem Soc 2000;21:383–8.

[26] Kalyuzhny G, Schneeweiss MA, Shanzer A, Vaskevich A, Rubinstein I. J Am Chem Soc 2001;123:3177–8.

[27] (a) Kalyanasundaram K, Thomas JK. J Am Chem Soc 1977;99:2039–44;
(b) Karpovich DS, Blanchard GJ. J Phys Chem 1995;99:3951–8.

[28] (a) Tedeschi C, Möhwald H, Kirstein S. J Am Chem Soc 2001;123:954–60;
(b) Chu DY, Thomas JK. Macromolecules 1987;20:2133–8.

[29] Claracq J, Santos SFCR, Duhamel J, Dumousseaux C, Corpart JM. Langmuir 2002;18:3829–35.

[30] Anghel DF, Toca-Herrera JL, Winnik FM, Rettig W, Klitzing RV. Langmuir 2002;18:5600–6.

[31] (a) Winnik FM. Chem Rev 1993;93:587–614;
(b) Siu H, Duhamel J. Macromolecules 2005;38:7184–6.

[32] (a) Todesco RV, Basheer RA, Kamat PV. Macromolecules 1986;19:2390–7;
(b) Winnik FM, Winnik MA, Tazuke S, Ober CK. Macromolecules 1987;20:38–44.